

ANCHORING METHODOLOGIES FOR PORE-SCALE NETWORK MODELS: APPLICATION TO RELATIVE PERMEABILITY AND CAPILLARY PRESSURE PREDICTION

Steven R McDougall, John Cruickshank, and Ken S Sorbie
Department of Petroleum Engineering
Heriot-Watt University
Edinburgh, EH14 4AS

ABSTRACT

The work described in this paper attempts to extend the predictive capability of pore-scale network models by using real experimental data as lithological "anchors". The development of such an anchored model capable of relative permeability and capillary pressure prediction would clearly be of great utility, providing a cheap and flexible tool for interpolating and extrapolating sparse and expensive laboratory data sets. Moreover, once the model had been anchored to reservoir rock samples, a wide range of sensitivities could be examined without recourse to additional experiments.

In the context of gas reservoir engineering, a preliminary methodology — utilising mercury injection capillary pressure (MICP) data — has been developed that could permit both the matching of existing experimental gas/oil relative permeability curves and the quantitative prediction of additional data sets. Two approaches have been considered. The first involves matching capillary pressure data from MICP experiments to extract pore size distribution and pore volume scaling information. These parameters are then used to *predict* the relative permeability curves directly. A second approach is to simply *match* the gas-oil relative permeability curves using a highly constrained bond model. Capillary pressure prediction is then treated as an inverse problem. The constrained set of adjustable parameters in the macropore network model comprises: coordination number (z), pore size distribution exponent (n), pore volume exponent (v) and pore conductivity exponent (λ) — i.e. only 4 simple parameters.

Results demonstrate that this basic four-parameter model is sufficient to reproduce the vast majority of experimental drainage relative permeability curves examined. Only one network simulation per sample is required to match both the wetting and non-wetting curves and each parameter obtained from the matching process lies within a narrow range of possible values. These highly encouraging results suggest that further over-parameterisation of the model is unnecessary in the context of drainage processes. However, we also show that anchoring network models to mercury intrusion data alone is insufficient for predicting relative permeabilities *a priori* — there is an interdependence of parameters and, consequently, an infinite set of parameter combinations will produce almost indistinguishable capillary pressure curves. Therefore, future analysis of MICP data should be performed in conjunction with the analysis of some other independent experiment — an experiment which gives one additional datum that forms the “missing

link” between anchoring and prediction. Some ideas relating to how this may best be achieved will be presented in this paper.

1. INTRODUCTION

Pore-scale network models offer an alternative approach towards the calculation of single and multiphase flow properties by explicitly incorporating interconnected pore elements into a three-dimensional framework. Network models were first suggested by Fatt in 1956 and his early model has been developed considerably over the intervening years (Chatzis & Dullien, 1977, 1985; Heiba *et al*, 1982; Mohanty & Salter, 1982, 1983; Jerauld & Salter, 1990; Blunt & King, 1990; McDougall & Sorbie, 1993, 1995, 1997; Øren *et al*, 1994, 1998). Indeed, the most recent models have extended the concept still further to the study of three-phase flow phenomena (Fenwick & Blunt, 1995; Mani & Mohanty, 1997; McDougall & Mackay, 1998) and even NMR responses in porous media (Damion *et al*, 2000).

Although a great deal of literature exists that corresponds to generic network modelling, relatively few attempts have been made to predict petrophysical parameters quantitatively. In fact, there has been a paucity of network studies incorporating any experimental data at all. The first attempt at fitting experimental relative permeability curves appears to have been undertaken by Lin and Slattery (1982), who had reasonable success in matching the capillary pressure and relative permeability data of Leverett (1939) with their 10-parameter model. Heiba *et al* (1992) used a Bethe lattice to approximate the porous medium and produced a good fit to the data of Talash (1976). Other studies include those of Bryant and Blunt (1992), Rajaram *et al* (1997) (in the context of unconsolidated soils) and Øren *et al* (1998). The latter authors extended the approach of Bryant and Blunt by incorporating models of sedimentation and diagenesis into the network reconstruction algorithm (in addition to the Bryant and Blunt compaction model). Capillary pressure and relative permeability predictions were presented and compared to two data sets. Whilst capillary pressures were well-matched in both cases, the large degree of scatter in the experimental core-flood data make relative permeability comparisons rather difficult. The mixed-wet system highlighted an interesting phenomenon: residual oil saturation initially increased with the fraction of oil-wet pores in the network, but decreased again once this fraction had exceeded some critical threshold. These findings successfully reproduce the earlier predictions of McDougall & Sorbie (1992), Dixit *et al* (1996), McDougall *et al* (1997) and Blunt (1997).

In this paper, the aim is to take a more direct modelling approach towards increasing the predictive capability of network models. Experimental data are used as lithological "anchors" and a preliminary methodology — utilising mercury injection capillary pressure (MICP) data — has been developed that could permit both the matching of existing experimental gas/oil relative permeability curves and the quantitative prediction of additional data sets. It is shown that, whilst experimental relative permeabilities can be matched relatively easily, anchoring network models to capillary pressure data is a necessary but not sufficient condition for accurate relative permeability *prediction* — the procedure is non-unique. The analysis presented here further demonstrates that if only one of the (n,v,z) parameters can be found by some other means, then this would provide the

“missing link” between data fitting and data prediction. Some ideas relating to how this may best be achieved are presented.

2. NETWORK MODELLING PRELIMINARIES

2.1. Introduction

Before describing the precise details of the anchoring procedure, it will be beneficial to briefly discuss some basic concepts relating to bond percolation models. In network models, the porous medium is modelled using a system of interconnected capillary elements, which generally configure to some known lattice topology. Although these network structures are somewhat idealised, the capillary radii are assigned randomly from a realistic pore size distribution in an effort to partially reconstruct the actual porous medium under investigation. Here, the porous medium is initially modelled using a three-dimensional cubic network of what will be referred to as *pore elements*. The various volume and conductivity functions associated with each element will be discussed later.

2.2. Basic Model

For the studies described here, the model used consisted of a three dimensional cubic network of capillary elements and elements can be randomly removed to simulate less well-connected systems. Using a Poiseuille-like flow law and invoking conservation of mass at each node leads to a set of linear pressure equations that can be solved to determine the nodal pressures. These, in turn, are used to calculate the elemental flows in each of the pore elements throughout the network

The simulation of capillary-dominated drainage processes is carried out using an invasion percolation model with hydraulic trapping of the wetting phase. More precise details of the model used in this work can be found elsewhere (eg. McDougall & Sorbie, 1997).

2.3. Inverse Capillary Pressure Plots

One of the main objectives of this study is to anchor network models using relatively cheap, easily-acquired experimental data and then to attempt to predict more complex petrophysical parameters such as relative permeabilities — mercury intrusion curves would be ideal candidates for this purpose. Although mercury/vacuum capillary pressure curves are often fairly structureless, their corresponding *R-plots* ($R=2\sigma\cos\theta/P_c$) have been shown to be more structured (McDougall and Sorbie, 1994). Consequently, *R-Plots* from the 8 reservoir samples were constructed from the intrusion data and the general form of these curves is shown schematically in Figure 1 — the initial steep decline is caused by the limited accessibility experienced by the mercury at the start of intrusion and the plateau region corresponds to the formation of a sample-spanning mercury cluster. Perhaps the most interesting aspect of these plots, however, is a clearly discernible point of inflection (kink) following the plateau regime. The structure of the *R-Plots* implies that most samples must contain an extremely large number of very small pores and/or a large volume fraction made up of pore corners and surface roughness. Hence, it may be supposed that the corresponding pore size distribution function to be used in the network flow analogue should also contain a large number of small pores (and that pore corner effects should also be included). The mercury injection simulator was consequently modified to incorporate cusped pore shapes (explicit corner porosity) and a Log-Uniform pore size distribution ($\sim 1/r$). None of the simulated *R-plots* exhibited the inflection point characteristic of

laboratory data, however, implying that neither continuous intrusion into pore edges nor a unimodal distribution function are sufficient *in themselves* to reproduce the kink effect. A modified approach must be considered and will be developed presently.

3. ANCHORING PROCEDURE

3.1. Fully Accessible Assumption

The simplest approach for simulating experimental mercury intrusion curves, in the R-plot form in particular, is the “3Rs” approach. This consists of building a network of pore elements, with each element assigned a radius, a volume and a conductance. The volume and conductance are considered to be proportional to the radius raised to some power, as follows:

$$\begin{aligned} P_c &\propto 1/r \\ v(r) &\propto r^n \\ g(r) &\propto r^l \end{aligned} \quad (1)$$

where P_c is the capillary pressure, $v(r)$ is the pore volume, and $g(r)$ the pore conductivity as a function of capillary entry radius, r . One extra constraint is added to the base case, which is that the pore radius distribution, $f(r)$, also has a power law dependence:

$$f(r) \propto r^n. \quad (2)$$

where $n < 0$ ($n > 0$) implies that there is a larger density of smaller (larger) pores and $n = 0$ implies a uniform distribution. Attention will initially be restricted to a unimodal distribution function. In reality, however, it is quite conceivable that rock samples will contain different families of pores; this possibility will be investigated later, when a bimodal model will be considered.

In investigating the base model, it is instructive to start with models that have perfect accessibility. The **accessibility** of a given pore network is given by $A(r)$ and measures the ratio of the number of invaded pores to the number that would have been invaded if each pore had a direct connection to the inlet. Thus, perfect accessibility is represented by $A(r) \equiv 1$. The effects of restricted accessibility will be considered later. The shape of the R-plot in the perfectly accessible case can be calculated analytically. Firstly, if r_{min} and r_{max} are the minimum and maximum radii of the distribution, we have;

$$S_{Hg}(r) = \int_r^{r_{max}} v(r)f(r) dr = \left(\frac{r_{max}^{n+n+1} - r^{n+n+1}}{r_{max}^{n+n+1} - r_{min}^{n+n+1}} \right) \quad (3)$$

Of course, the R-plot will always be monotonic with a negative gradient, but the second derivative will give more information about the shape of the curve;

$$\frac{dr}{dS_{Hg}} = - \frac{(r_{max}^{n+n+1} - r_{min}^{n+n+1})}{(n+n+1)} \cdot r^{-(n+n)} \quad (4)$$

$$\frac{d^2 r}{dS_{Hg}^2} = \frac{-(\mathbf{n} + n) \cdot (r_{\max}^{(\mathbf{n}+n+1)} - r_{\min}^{(\mathbf{n}+n+1)})}{(\mathbf{n} + n + 1)^2} \cdot r^{-(2\mathbf{n}+2n+1)} \quad (5)$$

Since r is always positive, we can see that if the sum of the exponents is positive, the slope of the curve will become steeper (more negative) with increasing r , which is defined as concave (a negative second derivative). Likewise, if the sum of the exponents is negative, the slope of the curve will decrease with r , giving a convex R -plot with a long tail. If the sum is zero, the R -plot will be a straight line. This result also demonstrates that the effects of the exponents \mathbf{n} and n are not unique, in that a change in one can be compensated for by an equivalent but opposite change in the other. Thus, the combination $\mathbf{n} = 1$ and $n = 2$ will give the same (normalised, $A(r) \equiv 1$) R -plot as for $\mathbf{n} = 2$ and $n = 1$. This non-uniqueness issue will be revisited in Section 5.

3.2. Inclusion of Accessibility

When the effect of accessibility is included in the R -plot, the shape is that predicted for perfect accessibility, multiplied by the accessibility function;

$$S_{Hg}(r) = A(r)S_{Hg}^{A=1}(r) \quad (6)$$

The accessibility function generally looks sigmoidal and the addition of accessibility creates a plateau region to the R -plot. The inclusion of accessibility effects can therefore produce portions of the same R -plot with concave and convex curvatures. Thus, the kind of R -plots which exhibit a shoulder or kink, and a tail region, as seen in most experimental curves, can be obtained with a negative $(\mathbf{n}+n)$ and restricted accessibility. However, some experimental data sets *cannot* be reproduced with the constrained 3Rs model described thus far, and the simple unimodal pore size model must be extended.

3.3. The Two Pore Family Model

An analytic form for the case in which there are two families of pores, with different volume and pore radius distribution exponents, should be capable of reproducing experimentally observed R -plots with long tails, a feature that we will subsequently ascribe to microporosity. One family describes all the pores above a critical radius, r_m and the other describes pores below this radius (i.e. the microporosity). The maximum radius is denoted by r_{\max} , while the minimum is r_{\min} . If the number fraction of pores in the second family (small pores) is given by \mathbf{a} , then;

$$\int_{r_{\min}}^{r_m} f(r) dr = \mathbf{a}, \quad \int_{r_{\min}}^{r_{\max}} f(r) dr = 1 \quad (7)$$

To satisfy these equations, it is found that;

$$\begin{aligned} f(r) &= \mathbf{j} \cdot r^{n_1} = \frac{(1-\mathbf{a})(n_1+1)}{(r_{\max}^{n_1+1} - r_{\mathbf{m}}^{n_1+1})} \cdot r^{n_1} & r_{\mathbf{m}} < r < r_{\max} \\ f(r) &= \mathbf{f} \cdot r^{n_2} = \frac{\mathbf{a}(n_2+1)}{(r_{\mathbf{m}}^{n_2+1} - r_{\min}^{n_2+1})} \cdot r^{n_2} & r_{\min} < r < r_{\mathbf{m}} \end{aligned} \quad (8)$$

Writing the volume functions as:

$$\begin{aligned} v(r) &= k_{v1} r^{n_1} & r_{\mathbf{m}} < r < r_{\max} \\ v(r) &= k_{v2} r^{n_2} & r_{\min} < r < r_{\mathbf{m}} \end{aligned} \quad (9)$$

the equation for $S_{Hg}(r)$ becomes:

$$S_{Hg}(r) = A(r) \frac{\mathbf{j} k_{v1} \left(\frac{r_{\max}^{n_1+n_1+1} - r^{n_1+n_1+1}}{\mathbf{n}_1 + n_1 + 1} \right)}{\mathbf{j} k_{v1} \left(\frac{r_{\max}^{n_1+n_1+1} - r_{\mathbf{m}}^{n_1+n_1+1}}{\mathbf{n}_1 + n_1 + 1} \right) + \mathbf{f} k_{v2} \left(\frac{r_{\mathbf{m}}^{n_2+n_2+1} - r_{\min}^{n_2+n_2+1}}{\mathbf{n}_2 + n_2 + 1} \right)} \quad (10)$$

for $r_{\mathbf{m}} < r < r_{\max}$, and

$$S_{Hg}(r) = A(r) \frac{\mathbf{j} k_{v1} \left(\frac{r_{\max}^{n_1+n_1+1} - r^{n_1+n_1+1}}{\mathbf{n}_1 + n_1 + 1} \right) + \mathbf{f} k_{v2} \left(\frac{r_{\mathbf{m}}^{n_2+n_2+1} - r^{n_2+n_2+1}}{\mathbf{n}_2 + n_2 + 1} \right)}{\mathbf{j} k_{v1} \left(\frac{r_{\max}^{n_1+n_1+1} - r_{\mathbf{m}}^{n_1+n_1+1}}{\mathbf{n}_1 + n_1 + 1} \right) + \mathbf{f} k_{v2} \left(\frac{r_{\mathbf{m}}^{n_2+n_2+1} - r_{\min}^{n_2+n_2+1}}{\mathbf{n}_2 + n_2 + 1} \right)} \quad (11)$$

for $r_{\min} < r < r_{\mathbf{m}}$

To complete the analysis, an analytic form for the accessibility function is required. This function depends on both the size of the network and the co-ordination number, z . By standardising on a 15x12x12 network, a family of curves was obtained, plotted as $A(p)$ versus p , where p is the *number fraction* that would have been invaded for the fully accessible case. These curves, obtained from network simulations, were used to test various analytic functions to find the one most appropriate to model the accessibility.

The most appropriate function was found to be:

$$A(p) = \frac{1}{1 + 10^4 \exp(kzp)} \quad (12)$$

The constant, k , can be found by considering the approximate relation at the 3D percolation threshold, $p_{\text{threshold}} \approx 1.5/z$, where $A(p)$ should equal 0.5 (by symmetry arguments). Thus, k is found to be -6.14 . Figure 2 compares the analytic accessibility function (Equation 12)

with that obtained from the 15x12x12 network model simulations. Expressing the accessibility function in terms of r rather than p , $A(r)$ is found to be:

$$A(r) = \frac{1}{1 + 10^4 \exp\left\{-6.14z(1-\mathbf{a})\left(\frac{r_{\max}^{n_1+1} - r^{n_1+1}}{r_{\max}^{n_1+1} - r_{\mathbf{m}}^{n_1+1}}\right)\right\}} \quad (13)$$

for $r_{\mathbf{m}} < r < r_{\max}$, and

$$A(r) = \frac{1}{1 + 10^4 \exp\left\{-6.14z\left((1-\mathbf{a}) + \mathbf{a}\left(\frac{r_{\mathbf{m}}^{n_2+1} - r^{n_2+1}}{r_{\mathbf{m}}^{n_2+1} - r_{\min}^{n_2+1}}\right)\right)\right\}} \quad (14)$$

and for $r_{\min} < r < r_{\mathbf{m}}$

3.4. Application to Experiment

Using the relations developed above (Equations 10, 11, 13 and 14), a spreadsheet was created to generate the R-plot resulting from the input parameters r_{\max} , $r_{\mathbf{m}}$, r_{\min} , n_1 , n_2 , \mathbf{n}_1 , \mathbf{n}_2 , \mathbf{a} , z , and the ratio k_{v1}/k_{v2} . Using this spreadsheet, it was possible to overlay the R-plots from the experimental data sets, and by adjusting the parameters, to find a close fit between the experimental and the model R-plots. The resulting R-plot comparisons are shown in Figure 3 (using the analytical model described above with two families of pores. Table 1 shows the parameters used to obtain the fits for these curves. z_L is the effective coordination number for the network of large pores alone ($R_{\mathbf{m}} < r < R_{\max}$).

Although excellent matches were obtained between the experimental and analytical R-plot curves, a more rigorous test of the procedure would be to use the anchored network to predict the corresponding relative permeabilities — this is considered next.

Important Note: Note that the accessibility effect (characterised by a large negative slope at low mercury saturations) is largely absent from some of the experimental data sets. This is primarily due to re-sampling and “clean-up” of some experimental data prior to supply to the authors. Moreover, no surface correction had been applied to the raw data — unfortunately, this raw data was unavailable to the authors and the model should not be expected to match the laboratory data in this region.

4. DIRECT PREDICTION OF RELATIVE PERMEABILITIES

In order to address the issue of relative permeability prediction, a decision was required concerning the network of microporosity. Although useful as a store of wetting fluid, the microporosity was not considered to play an important role in fluid transport. Consequently, pores belonging to the small pore family were removed from the network and flow calculations were restricted to the remaining macroscopic pores. Removal of the microporosity results in poorly connected macropore networks with $z < 4$. All of the

simulated networks were bonds-only models, and the 3Rs approach was used when assigning their properties.

Generally, direct relative permeability predictions assuming a fixed conductivity exponent of 3.0 were very poor (Figure 4), although the occasional data set was well-reproduced (Figure 4c). Slightly better predictions were produced when the conductivity exponent was allowed to vary from sample to sample and the results of Figure 4 are therefore rather pessimistic. Why should predictions from (apparently) well-anchored networks give such poor predictions? The results of Section 3 hold the key to answering this important question. That analysis clearly demonstrated that the shape of an R-plot is not *uniquely* defined in terms of a given combination of co-ordination number, volume exponent and pore size distribution exponent — different parameter combinations give identical R-plots. Given that laboratory flow data would be far more sensitive to some parameters (especially coordination number) than the static MICP data, it is perhaps not too surprising that the predicted relative permeabilities did not match the experimental values. However, from the work reported so far, it is still not clear whether the possibility exists that a consistent parameter set *could* be found that successfully reproduces both the R-plot and relative permeability data from experimental samples. In order to address this possibility, the inverse problem must be investigated.

5. THE INVERSE PROBLEM AND NON-UNIQUENESS

5.1. *The Inverse Problem*

An alternative approach to pore-scale anchoring is to simply *match* the gas-oil relative permeability curves using a highly constrained bond model. Capillary pressure prediction is then treated as an inverse problem. If good matches between simulation and experiment can be found using his procedure, then we know: (i) that it *is* possible to anchor a simple bond model to a reservoir sample, and (ii) that a consistent set of network parameters does exist that successfully reproduces both the R-plot and relative permeability data from experiment. Remember that the constrained set of adjustable parameters in the macropore model comprises only: coordination number (z), pore size distribution exponent (n), pore volume exponent (v) and pore conductivity exponent (λ).

Finding an optimised set of network parameters for each sample can be a time-consuming process, requiring many iterations based upon human judgement (although the whole process can be accelerated greatly if a close initial guess is possible). Since the results of many network simulations were already available to the authors, it made sense to utilise this information in a more systematic manner. To this end, an Artificial Neural Network (ANN) was developed using the parameterised relative permeability curves as inputs, and the network parameters as targets. This gave a way of obtaining a good initial estimate of the network parameters required to match a given pair of relative permeability curves.

Results of the inverse problem are shown in Figure 5 — both relative permeability and inverse capillary pressure results are shown. 5 sets of relative permeability simulations were performed using networks of dimensions 15x12x12 and differences in random number seed account for the scatter seen in each comparison. The parameter combinations required for each match are given in Table 2: values for conductivity exponent (not shown)

were highly constrained and in the range $\lambda \in [2.5, 4.0]$. These results clearly demonstrate that, for each data set, a consistent set of parameters *can* be found that reproduces both the gas/oil relative permeability curves *and* the mercury capillary pressure curve (although, for completeness, it should be noted that the occasional pathological case does exist). At first sight, this appears somewhat contradictory — how could a consistent match be found for the inverse problem but not for the original formulation? The answer lies in the fact that the experimental MICP data can be reproduced using many different model parameter combinations.

5.2. Non-Uniqueness

The analysis presented in Section 3 demonstrated that it is often possible to compensate for a change in one network parameter by adjusting the other two (from z , \mathbf{n} , and n), to obtain a very similar R-plot. Indeed, an example of this problem was seen when an artificial “experimental” R-plot was generated using a network model, and fits were attempted by an operator who was unaware of the network parameters used in the simulation. Even with such clean data, several possible fits could be obtained, making recovery of the exact values of the original parameters impossible. It is therefore very important to establish more rigorously the degree to which these parameters are interdependent.

An extension of the analysis given in Section 3 (for a unimodal distribution function) can be used to determine which parameter combinations will give similar shaped R-plots. Consider two networks with parameter combinations (n_1, v_1, z_1) and (n_2, v_2, z_2) . Examination of the second derivative shows that the curvature of the R-plot depends on the sum of \mathbf{n} and n (see earlier). Thus, to ensure that a second plot has the same curvature as the first, the new volume exponent must satisfy,

$$\mathbf{n}_2 = (\mathbf{n}_1 + n_1) - n_2 \quad (15)$$

Another constraint required for two R-plots to look similar is that they both have the same value of r at $A(r) = 1/2$ — this effectively correlates the two plateau regions. After a little algebra, this implies that z_2 must satisfy:

$$z_2 = \frac{3}{2} \cdot \frac{r_{\max}^{n_2+1} - r_m^{n_2+1}}{\left(r_{\max}^{n_2+1} - \left(r_{\max}^{n_1+1} - \frac{3}{2z_1} \cdot (r_{\max}^{n_1+1} - r_m^{n_1+1}) \right)^{\frac{n_2+1}{n_1+1}} \right)} \quad (16)$$

The significance of these equations is that a family of parameter triples can be determined that produce very similar R-plots but very *different* relative permeability curves. This answers the question posed at the end of Section 5.1 — it is obviously easier to find a consistent set of network parameters from the inverse problem. Hence, anchoring network models to capillary pressure data is a necessary but not sufficient condition for accurate relative permeability prediction — the procedure is non-unique.

6. CONCLUSIONS

The aim of this paper was to extend the predictive capability of pore-scale network models by using real experimental data as lithological "anchors". A more direct modelling approach was taken compared to that used elsewhere and a preliminary methodology — utilising mercury injection capillary pressure (MICP) data — was developed that could permit both the matching of existing experimental gas/oil relative permeability curves and the quantitative prediction of additional data sets. The main conclusion from this work were the following:

- Initially, a two pore-family model was used for anchoring purposes and 8 experimental data sets were considered. In all cases, a good match to the experimental MICP data was achieved, including that corresponding to microporosity.
- The results of direct gas/oil relative permeability predictions, however, were found to be generally poor and the anchored parameters differed from those required to match the relative permeability data directly.
- The inverse approach, whereby the relative permeability curves were matched and the R-plot was predicted, was far more successful. For each data set, a consistent set of parameters *could* be found that reproduced both the gas/oil relative permeability curves *and* the mercury capillary pressure curve. This implies that network models can be anchored to real experimental samples and used for subsequent sensitivity analyses (to flowrate and viscosity ratio, for example).
- Subsequent analysis showed that a family of (n,v,z) parameter triples could be determined that produce very similar R-plots but very *different* relative permeability curves. This explains why the inverse approach proved more successful.
- Hence, anchoring network models to capillary pressure data is a necessary but not sufficient condition for accurate relative permeability prediction — the procedure is non-unique.
- Analysis also shows that if only one of the (n,v,z) parameters could be found by some other means, then this would provide the “missing link” between data fitting and data prediction. Possible sources for this information may lie in mercury intrusion-extrusion loops, NMR T₂ distributions or thin section analysis — work in these areas is still ongoing.

REFERENCES

- Blunt, M.J. 1997. SPEJ (December), 449-.
- Blunt, M.J. & P. King. 1990. Phys. Rev. A, 42, 8, 4780.
- Bryant, S. & Blunt, M.J. 1992. Phys. Rev. A, 46, 2004-2011.
- Chatzis, I. & F.A.L. Dullien. 1977. J. Can. Pet. Technol. 16, 97-108.
- Damion, R.A, K.J. Packer, K.S. Sorbie, & S.R. McDougall. 2000. Chem. Eng. Sci., 55, 5981-5998.
- Dixit, A.B., S.R. McDougall, K.S. Sorbie, & J.S. Buckley. 1995. SPE 35451 presented at the 10th IOR Symposium.
- Fatt, I. 1956. Trans. AIME 207, 144-177.
- Fenwick, D.H. & M.J. Blunt. 1995. Proc. European IOR Symposium, Vienna.
- Heiba, A.A, M. Sahimi, L.E. Scriven, & H.T. Davis. 1982. SPE 11015 presented at the 1983 SPE ATCE.
- Jerauld, G.R. & S.J. Salter. 1990. Trans. Porous Media, 5, 103-151.
- Leverett, M.C. 1939. Trans. AIME 132, 149.
- Lin, C-Y. & J.C. Slattery. 1982. AIChE Journal Vol. 28(2), 311-323.
- McDougall, S.R. & K.S. Sorbie. 1993. SPE 25271 presented at the 68th SPE ATCE.
- McDougall, S.R. & K.S. Sorbie. 1995. SPE Reservoir Engineering (August).
- McDougall, S.R. & K.S. Sorbie. 1997. Petroleum Geoscience, 3, 161-169.
- McDougall, S.R. & K.S. Sorbie. 1992. Presented at ECMOR III, Delft.

- McDougall, S.R. Dixit, A.B. & K.S. Sorbie. 1997. From Lovell, M.A. & Harvey, P.K. (eds), Development in Petrophysics, Geological Society Special Publication No. 122.
- McDougall, S.R. & K.S. Sorbie. 1994. Presented at the DTI IOR Research Seminar, London.
- McDougall, S.R. & E.J. Mackay. 1998. Trans. IChemE, 76, (July).
- Mani, V. & K.K. Mohanty. 1997. J. Coll. Int. Sci., 187, 45.
- Mohanty, K. & S.J. Salter. 1982. SPE 11018 presented at the 57th SPE ATCE.
- Oren, P-E., S. Bakke, & O.J. Arntzen. 1998. SPEJ (December), 324-336.
- Rajaram, H., L.A. Ferrand, & M.A.Celia. 1997. Water Resour. Res., 33, 43-52.
- Talash, A.W. 1976. SPE 5810 presented at the 1976 Symposium on Improved Oil Recovery.

Table 1. Best fit parameters for freely fitted R -plots.

Sample	R_{max}	R_m	R_{min}	n_1	n_1	n_2	n_2	k_2/k_1	a	z	z_L
A	26.6	4	0.002	0.5	1	-0.7	0	4	0.37	6	3.78
B	18.1	4.5	0.002	1.6	1	-0.7	0	11.5	0.13	6	5.22
C	8.57	2	0.002	0	0.3	-1.25	0.5	5.5	0.38	5	3.1
D	11.85	2	0.002	-0.1	0.28	-0.9	0	1.3	0.48	6	3.12
E	8.2	1	0.002	-0.65	0	-0.65	0	1.25	0.41	6	3.54
F	6	3.5	0.002	2	3	-0.55	0	100	0.5	6	3
G	37.3	3	0.01	-0.95	0.1	-0.55	0	1	0.4	5	3
H	93.9	4	0.002	-0.95	0.85	-0.6	0	3.25	0.47	6	3.18

Table 2. The parameters used to obtain consistent fits of relative permeability and capillary pressure data.

Sample	R_{max}	R_μ	R_{min}	n_1	v_1	n_2	v_2	k_2/k_1	α	z	z_L
A	29	4	0.002	0	1	-0.8	0	4	0.333	6	4
B	23	4.5	0.002	0.2	1.2	-0.8	0	4.5	0.4	6	3.6
C	7	2	0.002	0	1	-0.75	0	4.75	0.333	6	4
D	11	2	0.002	-0.3	0.5	-0.85	0	3	0.367	6	3.8
E	5.8	2	0.002	-0.45	0.4	-0.65	0	3.4	0.433	6	3.4
F	6.4	4	0.002	0	0.9	-0.55	0	4.75	0.45	6	3.3
G	13	6.5	0.002	0	1.2	-0.7	0.2	85	0.175	4	3.3
H	80	5	0.002	-0.8	0.7	-0.5	0	2	0.5	6	3

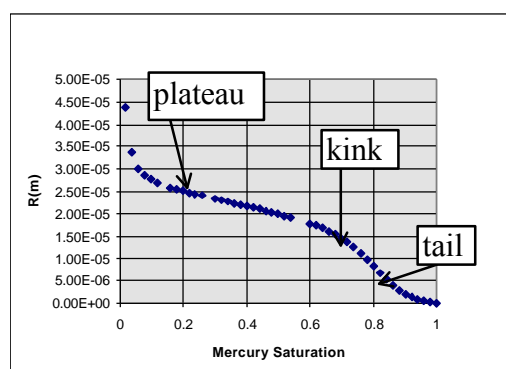


Figure 1. Schematic mercury intrusion data showing plateau, kink, and tail regions.

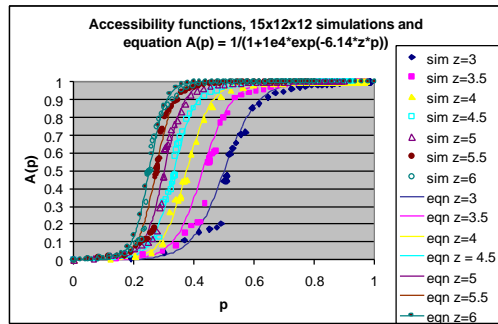


Figure 2. Accessibility functions obtained from network simulations compared to the analytic function found to best approximate the simulated results.

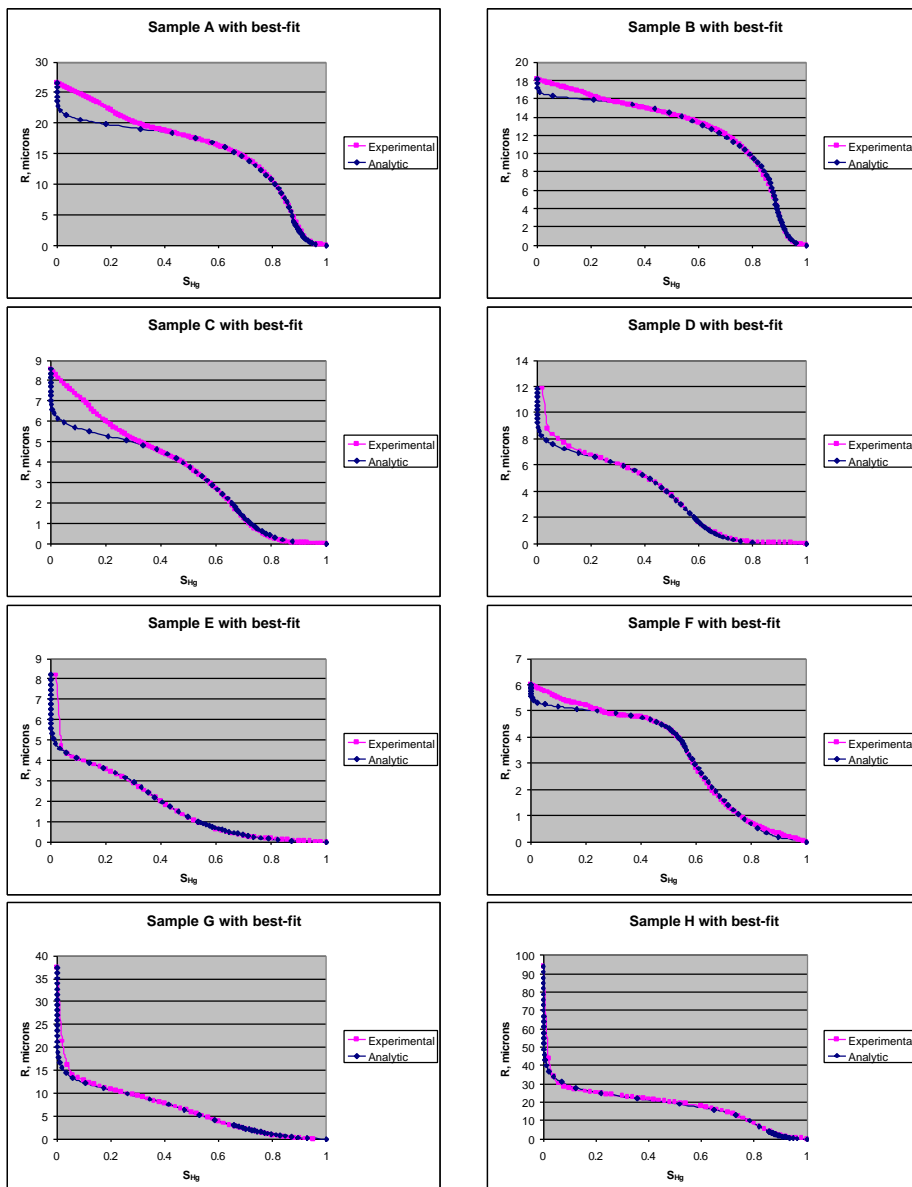


Figure 3. The best fit analytic R -plots for the two pore family model fitting the 8 sets of experimental data A-F.

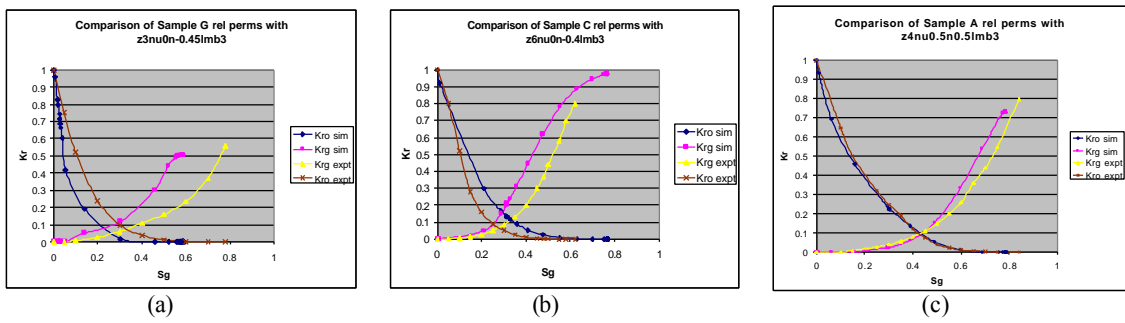
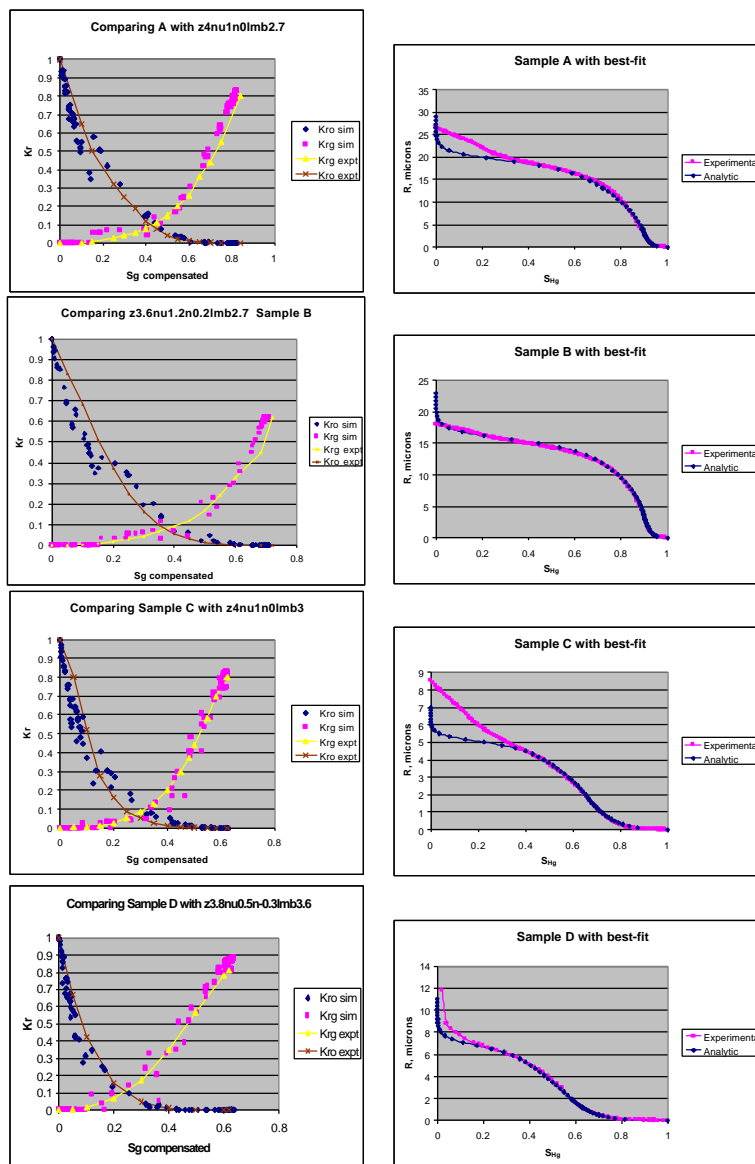


Figure 4. Direct predictions of gas-oil relative permeability curves using the parameter sets derived from R-plot fitting.



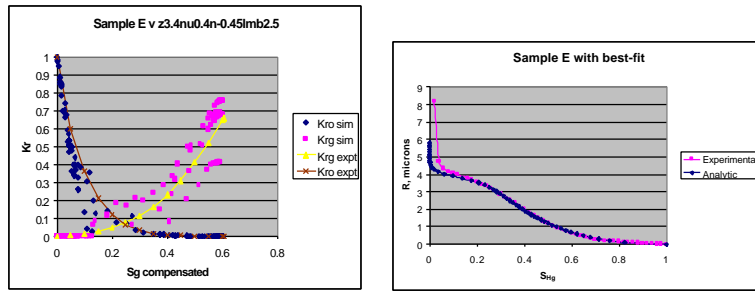


Figure 5. Consistent matches to gas-oil relative permeabilities and inverse capillary pressure data for reservoir samples A-E.

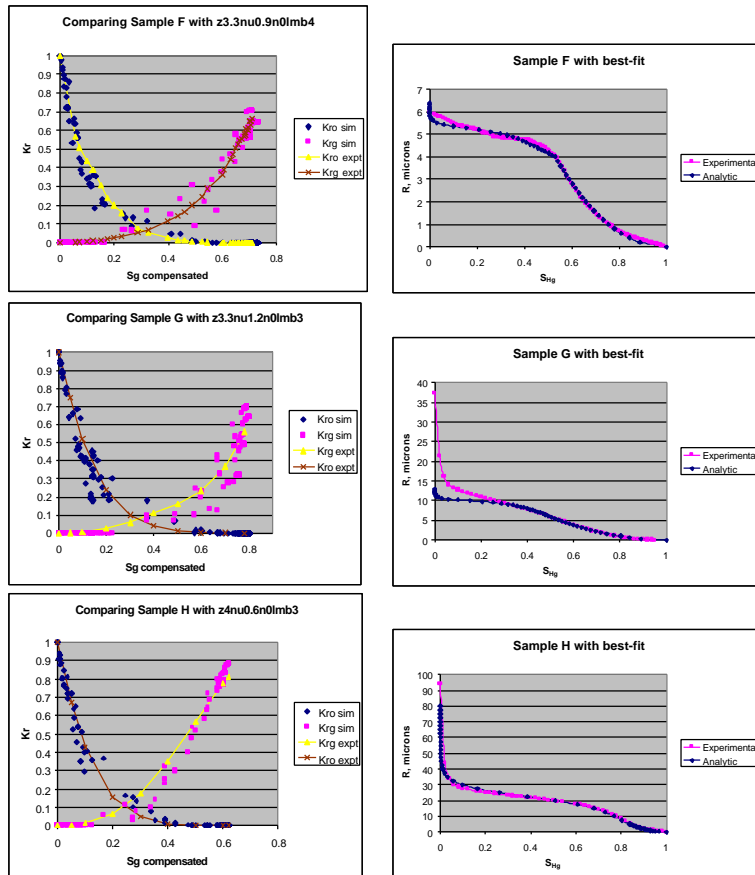


Figure 5 (cont.). Consistent matches to gas-oil relative permeabilities and inverse capillary pressure data for reservoir samples F-H.